Computational Models for Cylindrical Catalyst Particles

A study is made of computational methods for predicting the performance of cylindrical catalyst particles in reactions with nonlinear kinetics. Accurate two-dimensional collocation solutions are obtained and used to test simplified solution methods. A novel parametric integration method is used to traverse the region of multiple solutions. The local stability of several states is determined.

JAN P. SORENSEN
EARL W. GUERTIN
and
WARREN E. STEWART

Department of Chemical Engineering and Mathematics Research Center
University of Wisconsin
Madison, Wisconsin 53706

SCOPE

This paper deals with computational models for predicting the catalytic effectiveness of cylindrical particles. Such particles are commonly made by pelleting or by extrusion, with L/D from about 0.5 to 4. With the current trend towards realism in reactor modeling, a study of computational models for these important geometries is in order. Our goal here is to see under what conditions these two-dimensional particles can be adequately described by simple models.

Wheeler (1951) and Aris (1957) suggested that the effectiveness factor of a nonspherical particle could be estimated as that of a sphere with the same ratio of volume to external surface. This method works fairly well for linear reaction rate expressions but is open to question for nonlinear ones. We test the method here for nonlinear kinetics, using a first-order rate law with Arrhenius temperature dependence. This rate law exhibits a wide range of shapes, depending on the parameters γ and β of Equation (13).

Nonlinear kinetic models imply the possibility of multiple steady states of the reacting system. Luss and Amundson (1967a), Luss (1968, 1971), and Aris (1969) have used comparison theorems to predict when multiple solutions may occur. Stewart and Villadsen (1969) have obtained similar results by one-point orthogonal collocation. Here both approaches are compared with exact ignition and extinction limits for finite cylinders.

The tracing of the solution curves for finite cylinders is accomplished here by a novel method of parametric integration. The basic formulas, Equations (12) and (17), allow a predictor-corrector calculation which avoids error accumulation and yields accurate ignition and extinction points. The avoidance of cumulative error renders the method more stable than previous parametric integration procedures (Volkman and Kehat, 1969; Kubíček and Hlaváček, 1973).

CONCLUSIONS AND SIGNIFICANCE

The Wheeler-Aris shape correction with the sphere as the model shape predicts the steady state effectiveness factor within 5% for cylinders of L/D from 0.5 to 4 except near ignition or extinction limits. This method is expected to be satisfactory for most reaction rate expressions in view of the wide range of shapes included in Equation (13). Higher accuracy can be obtained when needed by the two-dimensional collocation method used in this paper.

Less accurate results are obtained when the slab or long cylinder is used as the model shape for the Wheeler-Aris method. Near the multiple-solution region, the effectiveness factors of finite cylinders can exceed all such predictions, whether based on slabs, spheres, or long cylinders.

One-point orthogonal collocation is simpler and more accurate than the Wheeler-Aris method for predicting ignition and extinction limits of finite cylinders. The bounds proposed by Luss (1968, 1971) are comparably accurate.

The parametric integration method used here appears to be widely applicable for tracing solutions of large systems of equations and determining how the solutions are connected. In this work, the method led to the discovery and identification of a second solution curve, which apparently disappears as the truncation error is decreased.

PROBLEM STATEMENT

Consider a cylindrical catalyst particle of length L and diameter D in which a single first-order chemical reaction is occurring. The temperature and concentrations are treated as constant over the external surface of the particle. We wish to study the internal transport and reaction by solving the dimensionless equations of continuity and energy

$$\frac{\partial z}{\partial \tau} = \frac{1}{r}\frac{\partial}{\partial r}\left(r\frac{\partial z}{\partial r}\right) + \frac{D^2}{L^2}\frac{\partial^2 z}{\partial x^2}$$

Correspondence concerning this paper should be addressed to W. E. Stewart.

$$- \phi^2 z \exp[(y-1)\gamma/y] \quad (1)$$

$$Le \frac{\partial y}{\partial \tau} = \frac{1}{r} \frac{\partial}{\partial r}\left(r \frac{\partial y}{\partial r}\right) + \frac{D^2}{L^2} \frac{\partial^2 y}{\partial x^2} + \phi^2 \beta z \exp[(y-1)\gamma/y] \quad (2)$$

under the boundary conditions:

$$\text{At} \quad r = 1 \quad \text{or} \quad x = 1: \quad z = 1 \quad \text{and} \quad y = 1 \quad (3, 4)$$

We use the usual conditions of finiteness of y and z and of symmetry about $r = 0$ and $x = 0$. Initial conditions consistent with these restrictions will be used below in analyzing the stability of some of the solutions. Our main interest, however, will be in the steady state solutions of Equations (1) to (4) and their use in testing simplified calculation methods.

In the steady state, Equations (2) and (4) may be replaced by the equation

$$y = 1 + (1 - z)\beta \quad (5)$$

derived by Prater (1958) for arbitrary geometry and kinetics. The steady state effectiveness factor is given by

$$\eta = 2 \int_0^1 \int_0^1 z \exp\left[\frac{\gamma\beta(1-z)}{1+\beta(1-z)}\right] r \, dr \, dx \quad (6)$$

in which Equation (5) has been used to eliminate the dimensionless temperature y from the reaction rate expression.

In place of the Thiele modulus ϕ, based on the particle radius R, Wheeler (1951) and Aris (1957) suggested using a modulus based on the dimension V_p/S_p in order to minimize the shape dependence of η. For cylinders with exposed ends, V_p/S_p becomes $R/(2 + D/L)$ whereas for spheres the value is $R/3$. Therefore, we use the modulus

$$\Lambda = \phi/(2 + D/L) \qquad \text{(cylinders)} \qquad (7a)$$

$$\Lambda = \phi/3 \qquad \text{(spheres)} \qquad (7b)$$

for presentation of the numerical solutions.

COLLOCATION EQUATIONS

The time-dependent Equations (1) to (4) can be solved numerically by orthogonal collocation over the interior of the particle. This involves the replacement of z and y by trial functions which exactly satisfy Equations (3) and (4), and adjusting the functions to satisfy Equations (1) and (2) at a set of interior collocation points (r_i, x_j). Here we use Equation (11) of Villadsen and Stewart (1967) to rewrite Equations (1) to (4) in terms of the concentrations and temperatures at the chosen points, and the computable weights B of their paper:

$$\frac{\partial z_{ij}}{\partial \tau} = \sum_{k=1}^{1+N_r} B_{ik,2}\, z_{kj} + \frac{D^2}{L^2} \sum_{k=1}^{1+N_x} B_{jk,1}\, z_{ik} - \phi^2 z_{ij} \exp[(y_{ij}-1)\gamma/y_{ij}] \begin{Bmatrix} i = 1, \ldots N_r \\ j = 1, \ldots N_x \end{Bmatrix} \quad (8)$$

$$Le \frac{\partial y_{ij}}{\partial \tau} = \sum_{k=1}^{1+N_r} B_{ik,2}\, y_{kj} + \frac{D^2}{L^2} \sum_{k=1}^{1+N_x} B_{jk,1}\, y_{ik} + \phi^2 \beta z_{ij} \exp[(y_{ij}-1)\gamma/y_{ij}] \begin{Bmatrix} i = 1, \ldots N_r \\ j = 1, \ldots N_x \end{Bmatrix} \quad (9)$$

$$\text{At} \quad i = 1 + N_r \quad \text{or} \quad j = 1 + N_x: \quad z_{ij} = 1 \quad \text{and} \quad y_{ij} = 1 \quad (10, 11)$$

This system of equations will be used below for stability analysis of the calculated steady states.

In the steady state, Equation (8) simplifies as follows with the use of Equation (5):

$$\sum_{k=1}^{1+N_r} B_{ik,2}\, z_{kj} + \frac{D^2}{L^2} \sum_{k=1}^{1+N_x} B_{jk,1}\, z_{ik} = \phi^2 f(z_{ij}) \begin{Bmatrix} i = 1, \ldots N_r \\ j = 1, \ldots N_x \end{Bmatrix} \quad (12)$$

Here $f(z)$ is the steady state rate function:

$$f(z) = z \exp\left[\frac{\gamma\beta(1-z)}{1+\beta(1-z)}\right] \quad (13)$$

Equation (12) yields an algebraic system of order $N_r N_x$; thus for $N_r = N_x = 6$ we get a system of 36 equations.

The effectiveness factor η is obtained from the solution values z_{ij} by numerical quadrature of the integral in Equation (6):

$$\eta = 2 \sum_{i=1}^{1+N_r} \sum_{j=1}^{1+N_x} W_{i,2}\, W_{j,1}\, f(z_{ij}) \quad (14)$$

The collocation points are situated to make this quadrature optimally accurate for polynomial integrands under the boundary conditions of Equations (3) and (4).

The solution for $N_r = N_x = 1$ is the simplest. In this case, Equations (12) and (14) become

$$[6 + 2.5(D/L)^2](1 - z_{11}) = \phi^2 f(z_{11}) \quad (15)$$

$$\eta = [5f(z_{11}) + 3]/8 \quad (16)$$

The solution is easily obtained graphically for given ϕ and L/D (as in Stewart and Villadsen, 1969) or by direct calculation for given z_{11}. Equation (15) works well for all values of L/D, but Equation (16) fails for L/D values far from unity where the polynomial quadrature becomes inappropriate for one of the coordinate directions.

SOLUTION OF THE COLLOCATION EQUATIONS

The system of Equations (12) is solvable by Newton's method, but the set of unknowns must be chosen with care. Ordinarily the solution is unique for given values of β, γ, and ϕ; however, in certain regions this choice leads to multiple solutions.

In this work, the multiple solution region was traversed by use of the derivative of Equation (12):

$$\sum_{k=1}^{1+N_r} B_{ik,2} \frac{dz_{kj}}{dz_{mn}} + \frac{D^2}{L^2} \sum_{k=1}^{1+N_x} B_{jk,1} \frac{dz_{ik}}{dz_{mn}} = \phi^2 \frac{df(z_{ij})}{dz_{mn}} + f(z_{ij}) \frac{d(\phi^2)}{dz_{mn}} \begin{Bmatrix} i = 1, \ldots N_r \\ j = 1, \ldots N_x \end{Bmatrix} \quad (17)$$

Here z_{mn} is the dimensionless concentration at a particular collocation point. This system of linear differential equations was integrated numerically with respect to z_{mn} starting from the following initial condition:

$$\text{At} \quad \phi = 0: \quad z_{ij} = 1 \quad \text{for all } i \text{ and } j \quad (18)$$

This represents the known, unique solution in the limit of small activity or small particle size. Equation (17) was used as a predictor and Equation (12) as a corrector to prevent accumulation of error.

Bifurcation points [where the multiplicity of solutions

TABLE 1. CALCULATED EFFECTIVENESS FACTORS FOR VARIOUS GEOMETRIES, WITH $\gamma = 30$

Values of η

β	Λ	$L/D = 0.$	$L/D = 0.5$	$L/D = 1.$	$L/D = 2.$	$L/D = 4.$	$L/D = \infty$	Sphere
−0.5	0.1	0.9512	0.9149	0.9116	0.9170	0.9228	0.9305	0.9195
	0.2	0.8424	0.7665	0.7610	0.7702	0.7806	0.7956	0.7747
	0.3	0.7270	0.6406	0.6353	0.6443	0.5549	0.6710	0.6490
	0.4	0.6271	0.5451	0.5406	0.5483	0.5577	0.5723	0.5525
	0.5	0.5457	0.4726	0.4689	0.4754	0.4834	0.4960	0.4790
	0.6	0.4803	0.4165	0.4134	0.4188	0.4256	0.4364	0.4219
	0.8	0.3840	0.3360	0.3337	0.3376	0.3428	0.3504	0.3398
	1.0	0.3180	0.2813	0.2796	0.2826	0.2868	0.2921	0.2842
	1.25	0.2608	0.2337	0.2325	0.2347	0.2382	0.2415	0.2357
	1.5	0.2205	0.2001	0.1990	0.2009	0.2039	0.2057	0.2014
	2.0	0.1680	0.1557	0.1548	0.1563	0.1590	0.1586	0.1562
	4.0	0.0854	0.0859	0.0852	0.0862	0.0882	0.0836	0.0847
0.0	0.1	0.9967	0.9936	0.9933	0.9938	0.9944	0.9950	0.9941
	0.2	0.9869	0.9752	0.9740	0.9759	0.9779	0.9805	0.9768
	0.3	0.9710	0.9466	0.9441	0.9481	0.9522	0.9575	0.9499
	0.4	0.9499	0.9104	0.9067	0.9128	0.9192	0.9277	0.9155
	0.5	0.9242	0.8694	0.8645	0.8726	0.8812	0.8928	0.8762
	0.6	0.8951	0.8261	0.8204	0.8299	0.8403	0.8546	0.8344
	0.8	0.8300	0.7400	0.7335	0.7445	0.7569	0.7749	0.7499
	1.0	0.7616	0.6614	0.6550	0.6659	0.6786	0.6978	0.6716
	1.25	0.6786	0.5779	0.5725	0.5821	0.5937	0.6120	0.5876
	1.5	0.6034	0.5101	0.5057	0.5138	0.5237	0.5400	0.5187
	2.0	0.4820	0.4103	0.4074	0.4129	0.4199	0.4318	0.4167
	4.0	0.2498	0.2269	0.2261	0.2278	0.2304	0.2338	0.2292
0.1	0.1	1.0067	1.0132	1.0139	1.0128	1.0116	1.0102	1.0123
	0.2	1.0278	1.0572	1.0606	1.0551	1.0496	1.0430	1.0528
	0.3	1.0663	1.1502	1.1614	1.1434	1.1265	1.1070	1.1361
	0.4	1.1284	1.3467	1.3791	1.3265	1.2771	1.2243	1.3049
	0.5	1.2273	1.6093	1.6119	1.6004	1.5546	1.4471	1.5823
	0.6	1.3901	1.6479	1.6219	1.6611	1.7000	1.7147	1.6731
	0.8	1.8799	1.4895	1.4666	1.5097	1.5621	1.6502	1.5366
	1.0	1.7530	1.3101	1.2943	1.3271	1.3680	1.4387	1.3527
	1.25	1.4396	1.125	1.116	1.136	1.170	1.2174	1.158
	1.5	1.2037	0.977	0.975	0.989	1.017	1.049	1.006
	2.0	0.903	0.773	0.766	0.787	0.795	0.819	0.793
	4.0	0.452	0.42	0.44	0.42	0.41	0.427	0.42
0.2†	0.1	1.0172	1.0346	1.0365	1.0333	1.0302	1.0263	1.0320
	0.2	1.0755	1.1833	1.1998	1.1737	1.1505	1.1252	1.1636
	0.3	1.2070	5.525	5.411	5.548	5.627	1.4618	5.558
	0.4	1.5826	5.434	5.538	5.568	5.811	6.3139	5.71
	0.5	7.2894	4.98	4.83	5.05	5.22	5.6120	5.17
	0.6	6.1021	4.49	4.42	4.44	4.69	4.951	4.66
	0.8	4.5784	3.5	3.7	3.7	3.9	3.96	3.7
	1.0	3.663	2.9	2.9	3.2	3.2	3.26	3.1
	1.25	2.93					2.6	
	1.5	2.45						
	2.0	1.82						
0.5	0.05	1.0119	1.0237	1.0250	1.0229	1.0208	1.0181	1.0220
	0.10	1.0509	1.1135	1.1217	1.1084	1.0960	1.0815	1.1031
	0.15	1.1300	1.4571	1.5898	1.4042	1.3116	1.2387	1.3598
	0.1518	1.1341	1.4959	1.8058*	1.4323	1.3267	1.2483	1.3809
	0.1609	1.1555			1.8104*	1.4246	1.3027	1.5331
	0.1664	1.1700				1.5175	1.3441	1.8806*
	0.1731	1.1892				1.8425*	1.4062	
	0.1936	1.2625					2.0859*	
	0.2562	2.3782*						

† The values below the ruled line for $\beta = 0.2$ represent ignited states.
* Ignition points.

$z_{ij}(\phi)$ changes] were detected readily by the resulting sign change of $d(\phi^2)/dz_{mn}$. Quadratic interpolation on this derivative was used for accurate calculation of these points.

The integral path of Equation (17) will be unique provided that the rank of the N by $N + 1$ matrix of coefficients remains equal to N along the path. This condition was demonstrated here by choosing a variable z_{mn} for which the determinant of the system never changed sign; the existence of such a variable is sufficient for uniqueness but not necessary. Thus, the solutions $z_{ij}(z_{mn})$, $\phi^2(z_{mn})$, and $\eta(z_{mn})$ were unique for each initial condition, even when $\eta(\phi)$ was multivalued.

Table 1 gives the calculated effectiveness factors η as functions of Λ and β for several catalyst shapes. Our purpose is not to give a complete mapping, but rather to provide data for comparison with approximate predictions. The results are calculated with $N_x = N_r = 6$, except

that $N = 8$ was used for the slab, long cylinder, and sphere in the ignited region. The results are usually accurate to the last digit.

For strongly exothermic reactions (large positive β and γ), *the solution* for $\eta(\Lambda)$ is multivalued in a certain range $\Lambda_{min} \leq \Lambda \leq \Lambda_{max}$, where Λ_{min} and Λ_{max} are the extinction and ignition points. The limits of this region are shown in Figures 1 to 3, and accurate values are given in Table 2. The exact results for slabs ($L/D = 0$) are consistent with those of Drott and Aris (1969); their Equations (21) and (22) should be multiplied on the right by $1/\beta$ and β respectively to agree with their tables. The exact results for spheres are consistent with those of Luss (1971) and of Weisz and Hicks (1962). The results for nonisothermal cylinders are new.

The effectiveness factors $\eta(\Lambda)$ for cylinders are nearly independent of L/D over the range $0.5 \leq L/D \leq 4$, except for conditions near the multivalued region (which in practice should be avoided). With the same restrictions, $\eta(\Lambda)$ is nearly the same for short cylinders as for spheres. Thus the dependence of η on L and D is well predicted by taking η for a sphere with the same characteristic dimension V_p/S_p, as proposed by Wheeler (1951) and Aris (1957). This prediction method is asymptotically correct when Λ is very small or very large. Luss and Amundson (1967b) showed that η varies strongly with L/D when $(V_p)^{1/3}$ is used in place of V_p/S_p as the characteristic dimension.

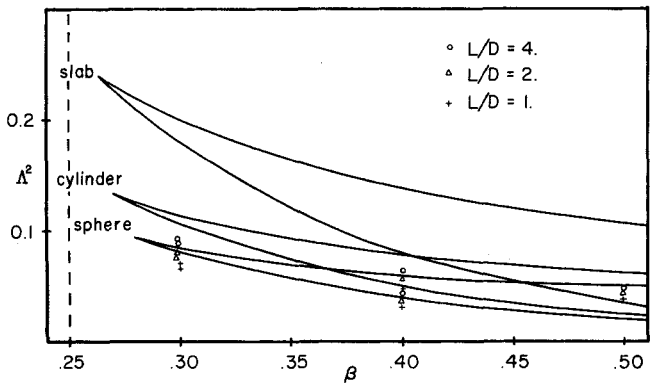

Fig. 1. Limits of multiple solution region for $\gamma = 20$. The curves are the limits for the slab, cylinder and sphere; the points are the limits for short cylinders. The vertical dotted line is the minimum β for multiple solutions according to Equation (21).

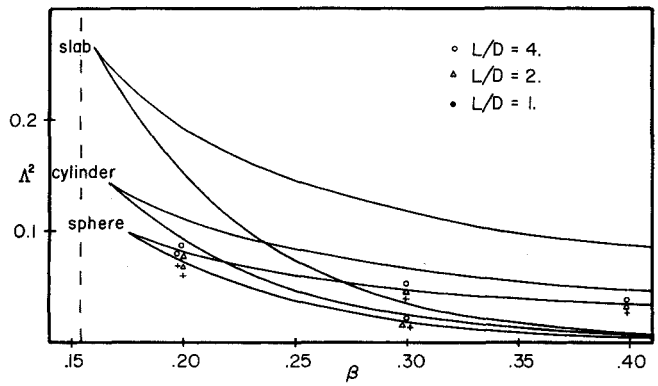

Fig. 2. Limits of multiple solution region for $\gamma = 30$.

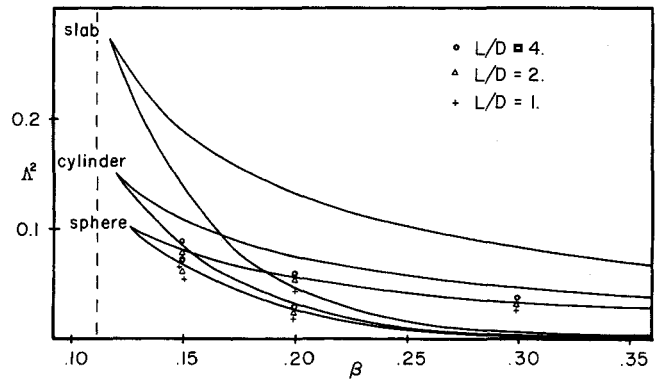

Fig. 3. Limits of multiple solution region for $\gamma = 40$.

SIMPLE EXPRESSIONS FOR MULTIPLE-SOLUTION LIMITS

Equation (15) allows a simple treatment of multiple-solution limits. It is useful to do this first and then to compare the results with detailed analyses of Equations (1) to (4).

The solution of Equation (15) for z is unique at each value of ϕ if and only if

$$\frac{d}{dz}\left[\frac{f(z)}{1-z}\right] > 0 \quad \text{for} \quad 0 < z < 1 \qquad (19)$$

This condition has been shown by Luss (1968, 1971) and Aris (1969) to be sufficient for uniqueness of the steady state solution of Equations (1) to (4) as well.

Multiple roots of Equation (15) occur at points where $f(z)/(1-z)$ reaches a locally stationary or extremal value. These are the bifurcation points of the solution locus $z_{11}(\phi)$. The solution $z_{11}(\phi)$ is multivalued between the largest and smallest multiple roots, z_{max} and z_{min}.

If $f(z)$ and $f'(z)$ are continuous, z_{max} and z_{min} may be found by setting $d[f(z)/(1-z)]/dz$ equal to zero. For $f(z)$ of Equation (13), this gives

$$z^2(\beta\gamma + \beta^2) - z(\beta\gamma + 2\beta^2 + 2\beta) + (1+\beta)^2 = 0 \qquad (20)$$

The roots of this equation,

$$z = \frac{(\beta\gamma + 2\beta^2 + 2\beta) \pm \sqrt{\beta\gamma(\beta\gamma - 4\beta - 4)}}{2(\beta\gamma + \beta^2)} \qquad (21)$$

if real, are the values of z_{max} and z_{min} for the given β and γ.

Distinct roots z_{max} and z_{min} occur whenever the discriminant in Equation (21) is positive. Insertion of these roots in Equation (15) gives the following multiple-solution limits:

$$\phi^2_{max,1} = [6 + 2.5(D/L)^2]\,(1 - z_{max})/f(z_{max}) \qquad (22)$$

$$\phi^2_{min,1} = [6 + 2.5(D/L)^2]\,(1 - z_{min})/f(z_{min}) \qquad (23)$$

Table 2 shows these results along with the true limiting solutions of Equations (1) to (4). The agreement is good for Λ_{max} and reasonable for Λ_{min}; note that Equations (22) and (23) bracket the true multiple-solution region in all cases considered here.

Luss (1971) has given related expressions for ϕ_{max} and ϕ_{min} and has tested them for slabs and spheres. With small notational changes, his results can be written

$$\phi^2_{max} < \mu_1^2(1 - z_{max})/f(z_{max}) \quad \text{(proved for slabs)} \qquad (24)$$

$$\phi^2_{min} > \mu_1^2(1 - z_{min})/f(z_{min}) \quad \text{(empirical)} \qquad (25)$$

$$\phi^2_{min} > \lambda^2(1 - z_{min})/f(z_{min}) \quad \text{(proved for all geometries)} \qquad (26)$$

Table 2a. Calculated Ignition Limits, Λ_{max}

γ	β	Method*	$L/D=0$	$L/D=1$	$L/D=2$	$L/D=4$	$L/D=\infty$	Sphere
20.	0.30	Eq. (22)	0.4546	0.2794	0.2960	0.3170	0.3521	0.3105
		Exact	0.4460	0.2660	0.2815	0.3024	0.3378	0.2914
	0.40	Eq. (22)	0.3786	0.2327	0.2465	0.2640	0.2932	0.2586
		Exact	0.3709	0.2204	0.2334	0.2509	0.2804	0.2415
	0.50	Eq. (22)	0.3320	0.2041	0.2162	0.2315	0.2572	0.2268
		Exact	0.3251	0.1930	0.2044	0.2198	0.2457	0.2115
30.	0.20	Eq. (22)	0.4470	0.2747	0.2911	0.3118	0.3462	0.3054
		Exact	0.4380	0.2604	0.2758	0.2964	0.3313	0.2853
	0.30	Eq. (22)	0.3485	0.2142	0.2269	0.2431	0.2699	0.2381
		Exact	0.3411	0.2023	0.2143	0.2305	0.2577	0.2217
	0.40	Eq. (22)	0.2960	0.1819	0.1927	0.2064	0.2293	0.2022
		Exact	0.2896	0.1717	0.1819	0.1956	0.2187	0.1881
	0.50	Eq. (22)	0.2619	0.1610	0.1705	0.1827	0.2029	0.1789
		Exact	0.2562	0.1518	0.1609	0.1731	0.1935	0.1664
40.	0.15	Eq. (22)	0.4435	0.2726	0.2888	0.3093	0.3436	0.3030
		Exact	0.4344	0.2580	0.2732	0.2938	0.3283	0.2827
	0.20	Eq. (22)	0.3712	0.2281	0.2417	0.2589	0.2875	0.2536
		Exact	0.3632	0.2154	0.2281	0.2454	0.2744	0.2360
	0.30	Eq. (22)	0.2944	0.1809	0.1917	0.2053	0.2280	0.2011
		Exact	0.2879	0.1706	0.1807	0.1944	0.2174	0.1870

Table 2b. Calculated Extinction Limits, Λ_{min}

γ	β	Method*	$L/D=0$	$L/D=1$	$L/D=2$	$L/D=4$	$L/D=\infty$	Sphere
20.	0.30	Eq. (23)	0.4209	0.2587	0.2741	0.2935	0.3260	0.2875
		Exact	0.4233	0.2616	0.2766	0.2963	0.3269	0.2863
	0.40	Eq. (23)	0.2709	0.1665	0.1764	0.1889	0.2098	0.1851
		Exact	0.2791	0.1817	0.1929	0.2077	0.2212	0.1984
	0.50	Eq. (23)	0.1791	0.1101	0.1166	0.1249	0.1387	0.1223
		Exact	0.1879	0.1272	0.1357	0.1469	0.1520	0.1385
30.	0.20	Eq. (23)	0.3826	0.2351	0.2491	0.2668	0.2963	0.2614
		Exact	0.3888	0.2452	0.2595	0.2787	0.3034	0.3682
	0.30	Eq. (23)	0.1732	0.1064	0.1128	0.1208	0.1341	0.1183
		Exact	0.1840	0.1273	0.1359	0.1461	0.1508	0.1383
	0.40	Eq. (23)	0.0830	0.0510	0.0541	0.0579	0.0643	0.0567
		Exact	0.0911	0.0671	0.0716	0.0755	0.0774	0.0718
	0.50	Eq. (23)	0.0429	0.0264	0.0279	0.0299	0.0332	0.0293
		Exact	0.0481	0.0369	0.0415	0.0407	0.0418	0.0397
40.	0.15	Eq. (23)	0.3609	0.2218	0.2350	0.2517	0.2795	0.2465
		Exact	0.3691	0.2357	0.2496	0.2683	0.2898	0.2576
	0.20	Eq. (23)	0.2002	0.1231	0.1304	0.1396	0.1551	0.1368
		Exact	0.2123	0.1460	0.1557	0.1676	0.1735	0.1587
	0.30	Eq. (23)	0.0647	0.0397	0.0421	0.0451	0.0501	0.0442
		Exact	0.0725	0.0551	0.0619	0.0612	0.0629	0.060

* Exact values were obtained by orthogonal collocation with 6 collocation points along each coordinate.

Table 3. Comparison of Predicted Multiple-Solution Limits, Equations (22) to (26)

	$L/D=0$	0.5	1.0	2.0	4.0	∞	Sphere
μ_1^2	$2.467\ D^2/L^2$	15.65	8.25	6.40	5.94	5.78	π^2
λ^2	$2\ D^2/L^2$	9.86	4.98	4.07	4.00	4.00	6.00
$\mu_1^2/[6+2.5\,(D/L)^2]$	0.994	0.989	0.985	0.984	0.982	0.982	0.970

To apply these expressions in two dimensions we need to calculate the eigenvalues μ_1^2 and λ^2. For finite cylinders we obtain

$$\mu_1^2 = \left[(2.4048\ldots)^2 + \left(\frac{\pi D}{2L}\right)^2 \right] \qquad (27)$$

and our results for λ^2 are given in Table 3.

Equations (24) and (25) agree closely with (22) and (23), as can be seen from Table 3. The agreement for all geometries shown is within 3%. The bound in Equation (26) is not as close as the prediction of Equation (25) for these geometries.

Equations (22) to (26) can be extended to variable effective diffusivities by use of a transformed concentration in the manner of Stewart and Villadsen (1969). Our Equation (15) can be obtained from their Equation (16)

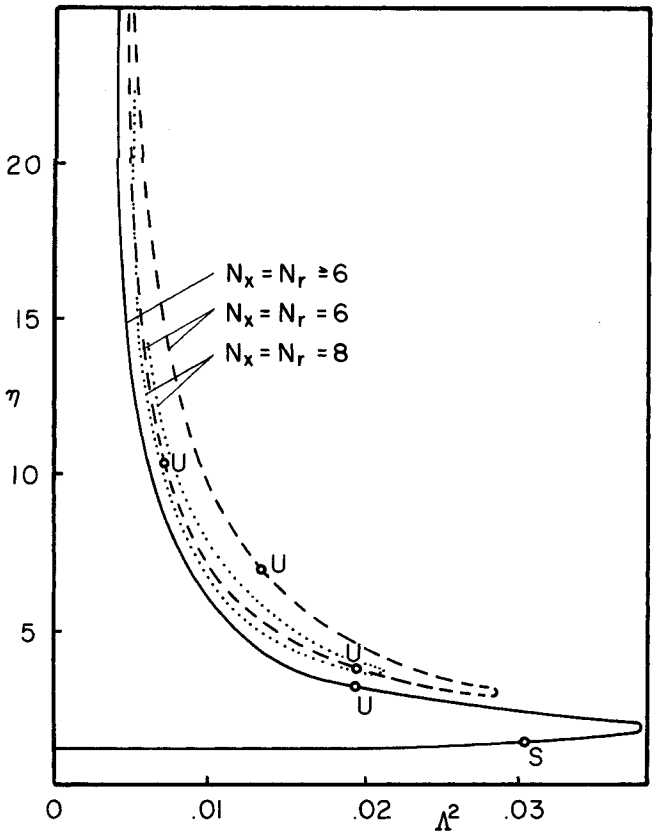

Fig. 4. Integral curves in the multiple-solution region for cylinders with $\beta = 0.3$, $\gamma = 40$ $L/D = 4$. Point S is stable for all Lewis numbers; points U are unstable for all Lewis numbers.

by the substitution $1/l^2 = 10/L^2 + 24/D^2$ for finite cylinders.

CONNECTEDNESS AND STABILITY OF SOLUTIONS

The parametric integration of Equation (17) led to an unusual result for $\beta = 0.3$ and $\gamma = 40$, with $L/D = 4$. With $N_r = N_x = 6$, two solution curves $\eta(\Lambda)$ were obtained, as shown in Figure 4. The solid curve is the solution for sufficiently small Δz_{mn}, starting from $\eta = 1$ at $\Lambda = 0$ and continuing through the multiple solution region. The dashed curve is part of a closed loop obtained by integrating Equation (17) from a point accidentally reached when using a large increment Δz_{mn}. The curves are distinct since Equation (17) has full rank on each and thus gives a unique tangent line at every point.

To check these results, new traverses were made with $N_r = N_x = 8$. The solid curve was essentially duplicated, but the loop curve changed significantly as shown by the dotted curve on Figure 4. From this we conclude that the loop curve is a parasitic solution, which apparently would disappear at a somewhat higher order of collocation.

The local stability of these solutions was investigated at the points shown in Figure 4 by linearizing Equations (8) and (9) and computing the eigenvalues of the resulting system of ordinary differential equations. The point labeled S is stable (all eigenvalues negative) for all Lewis numbers. The points labeled U are unstable for all Lewis numbers.

These results illustrate the importance of checking the stability of solutions of nonlinear problems. They also show the utility of parametric integration in tracing out the solution curves.

ACKNOWLEDGMENT

This work was supported by the National Science Foundation (Grant GK-17860) and by the University of Wisconsin Mathematics Research Center, sponsored by the United States Army under Contract No. DA-31-124-ARO-D-462.

NOTATION

$B_{ij,a}$ = weights for expressing $u^{1-a}\frac{d}{du}\left(u^{a-1}\frac{dg}{du}\right)$ at $u = u_i$ in terms of ordinates $g(u_j)$

D = diameter of cylinder or sphere, m

$\mathcal{D}_{eff}$ = effective diffusivity of reactant in particle, $m^2\ s^{-1}$

E/R = activation energy, K

$f(z)$ = reaction rate function, normalized to unity at $z = 1$, Equation (13)

ΔH = enthalpy of reaction, J $kmol^{-1}$

k_{eff} = effective thermal conductivity, J $s^{-1}\ m^{-1}\ K^{-1}$

k_0 = reaction rate constant at temperature T_0, s^{-1}

L = length of cylinder, m

Le = $\left(\frac{\mathcal{D}\rho\hat{C}_p}{k\epsilon}\right)_{eff}$, modified Lewis number

N = total number of collocation points

N_k = number of collocation points in coordinate k

R = radius of cylinder or sphere, m

r = dimensionless radial coordinate

S_p = outer surface area of particle, m^2

t = time, s

V_p = volume of particle, m^3

x = dimensionless length coordinate

y = T/T_0, dimensionless temperature

z = c/c_0, dimensionless concentration

$W_{i,a}$ = integration weights for expressing $\int_0^1 g(u)\,u^{a-1}\,du$ in terms of ordinates $g(u_i)$

Greek Letters

β = $\frac{-\Delta H\,\mathcal{D}_{eff}\,c_0}{k_{eff}\,T_0}$, dimensionless coefficient in Equation (2)

γ = $\frac{E}{R\,T_0}$, dimensionless coefficient in Equations (1) and (2)

ϵ = effective void fraction for reactant, including adsorption on pore walls

η = effectiveness factor

Λ = $\frac{V_p}{S_p}\sqrt{\frac{k_0}{\mathcal{D}_{eff}}}$

λ^2 = $1/v_{max}$, where v is the solution of $R^2\nabla^2 v = -1$ in the given particle with $v = 0$ on the outer surface

μ_1^2 = dominant eigenvalue of $R^2\nabla^2 v + \mu_1^2 v = 0$ in the given particle with $v = 0$ on the outer surface

$(\rho\hat{C}_p)_{eff}$ = combined heat capacity of solid and fluid, J $m^{-3}\ K^{-1}$

τ = $\frac{\mathcal{D}_{eff}\,t}{\epsilon R^2}$, dimensionless time

ϕ = $R\sqrt{\frac{k_0}{\mathcal{D}_{eff}}}$, Thiele modulus

Subscripts

a = geometric parameter: 1 for rectangular coordi-

nate, 2 for radial cylindrical coordinate, and 3 for radial spherical coordinate

min, max = limits of particle size modulus for multiple solution region

0 = outer surface

1 = first collocation approximation, or first eigenvalue

LITERATURE CITED

Aris, R., "On Shape Factors for Irregular Particles—I. The Steady State Problem. Diffusion and Reaction," *Chem. Eng. Sci.*, **6**, 262 (1957).

———., "On Stability Criteria of Chemical Reaction Engineering," *ibid.*, **24**, 149 (1969).

Drott, D. W., and R. Aris, "Communications on the Theory of Diffusion and Reaction—I. A Complete Parametric Study of the First-Order, Irreversible Exothermic Reaction in a Flat Slab of Catalyst," *ibid.*, **24**, 541 (1969).

Kubicek, M., and V. Hlavacek, "Solution of Nonlinear Boundary Value Problems—VII. A Novel Method: Differentiation with Respect to Boundary Condition," *ibid.*, **28**, 1049 (1973).

Luss, D., "Sufficient Conditions for Uniqueness of the Steady State Solutions in Distributed Parameter Systems," *ibid.*, **23**, 1249 (1968).

———., "Uniqueness Criteria for Lumped and Distributed Parameter Chemically Reacting Systems," *ibid.*, **26**, 1713 (1971).

———., and N. R. Amundson, "Uniqueness of the Steady State Solutions for Chemical Reaction Occurring in a Catalyst Particle or in a Tubular Reactor with Axial Diffusion," *ibid.*, **22**, 253 (1967a).

———., "On a Conjecture of Aris: Proof and Remarks," *AIChE J.*, **13**, 759 (1967b).

Prater, C. D., "The Temperature Produced by Heat of Reaction in the Interior of Porous Particles," *Chem. Eng. Sci.*, **8**, 284 (1958).

Stewart, W. E., and J. V. Villadsen, "Graphical Calculation of Multiple Steady States and Effectiveness Factors for Porous Catalysts," *AIChE J.*, **15**, 28 (1969).

Villadsen, J. V., and W. E. Stewart, "Solution of Boundary-Value Problems by Orthogonal Collocation," *Chem. Eng. Sci.*, **22**, 1483 (1967); **23**, 1515 (1968).

Volkman, Y., and E. Kehat, "Computation of Effectiveness Factors," *ibid.*, **24**, 1531 (1969).

Weisz, P. B., and J. S. Hicks, "The Behaviour of Porous Catalyst Particles in View of Internal Mass and Heat Diffusion Effects," *ibid.*, **17**, 265 (1962).

Wheeler, A., "Reaction Rates and Selectivity in Catalyst Pores," *Advan. Catalysis*, **3**, 249, 294 (1951).

Manuscript received March 29, 1973; revision received and accepted May 22, 1973.

A Stochastic Analysis of a Nonisothermal Packed Bed Reactor

Monte Carlo techniques have been used to simulate the stochastic responses of the nonisothermal packed bed reactor. Random variables with specified ensemble means, ensemble standard deviations, and probability distributions (normal, uniform, or autocorrelated) were introduced as inputs and parameters into the model equations, and the equations were solved repeatedly to provide a sample of the outputs. Sample means and sample standard deviations both in the steady and unsteady state were evaluated and the probability distributions of the output temperature and concentration characterized. Confidence limits for a specified confidence coefficient have been determined from which overdesign factors could be computed.

T. KADO
and
D. M. HIMMELBLAU

Department of Chemical Engineering
The University of Texas
Austin, Texas 78712

SCOPE

In formulating a mathematical model of a process, two different approaches can be discerned: one is deterministic and the other stochastic. In a stochastic model a knowledge of the state of the variables and parameters at some moment in time no longer uniquely determines the state of the parameters at succeeding times. Stochastic models are, in general, more difficult to work with than deterministic models, but in many cases they can provide more insight into the characteristics and behavior of a real process.

Unfortunately, but not unexpectedly, the formulation of the more representative stochastic models of reactors results in equations whose dependent variables are non-Markovian, nonstationary or both. Consequently, while it is usually not too difficult to write down the basic (differential) equations describing a packed bed reactor, how to obtain a complete, partial, or approximate analytical solution for a stochastic reactor model is a stumbling block. Most of the published work on reactor models has been limited to the somewhat unrealistic case in which the random coefficients and inputs are white noise because then analytical solutions can be found.